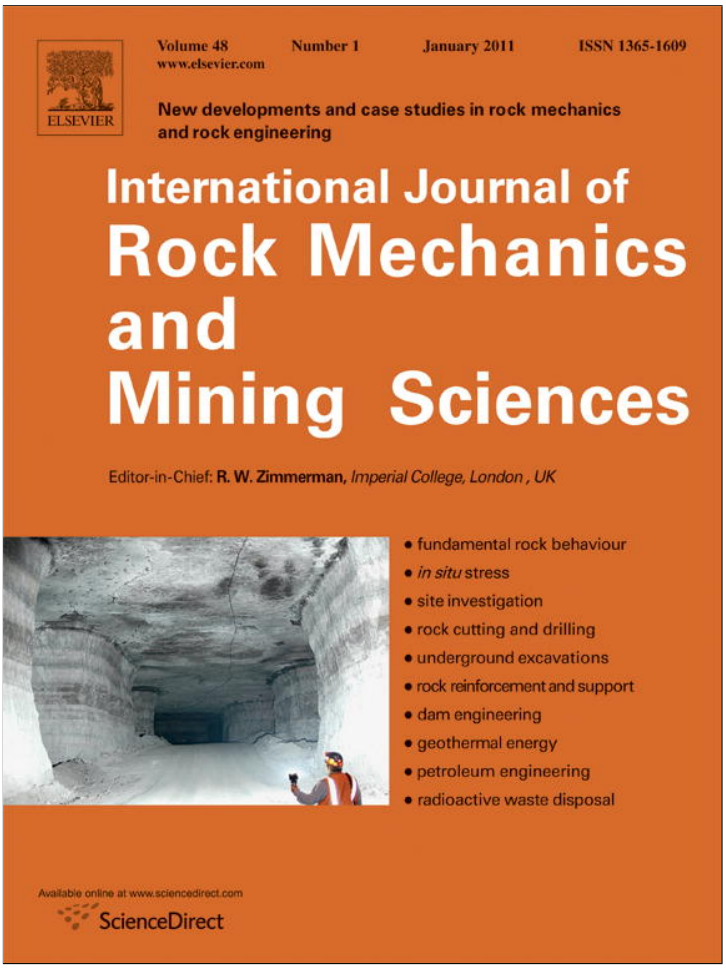

International Journal of Rock Mechanics & Mining Sciences 48 (2011) 27–41

Contents lists available at ScienceDirect

International Journal of Rock Mechanics & Mining Sciences

journal homepage: www.elsevier.com/locate/ijrmms

Probabilistic modeling using bivariate normal distributions for identification of flow and displacement intervals in longwall overburden

C. Özgen Karacan*, Gerrit V.R. Goodman

NIOSH, Office of Mine Safety and Health Research, Pittsburgh, PA 15236, USA

ARTICLE INFO

Article history:
Received 27 November 2009
Received in revised form
18 June 2010
Accepted 14 August 2010
Available online 1 September 2010

Keywords:
Longwall overburden
Gob gas ventholes
Bivariate normal distribution
Conditional probability

ABSTRACT

Gob gas ventholes (GGV) are used to control methane emissions in longwall mines by capturing it within the overlying fractured strata before it enters the work environment. In order for GGVs to effectively capture more methane and less mine air, the length of the slotted sections and their proximity to top of the coal bed should be designed based on the potential gas sources and their locations, as well as the displacements in the overburden that will create potential flow paths for the gas.

In this paper, an approach to determine the conditional probabilities of depth-displacement, depth-flow percentage, depth-formation and depth-gas content of the formations was developed using bivariate normal distributions. The flow percentage, displacement and formation data as a function of distance from coal bed used in this study were obtained from a series of borehole experiments contracted by the former US Bureau of Mines as part of a research project. Each of these parameters was tested for normality and was modeled using bivariate normal distributions to determine all tail probabilities. In addition, the probability of coal bed gas content as a function of depth was determined using the same techniques. The tail probabilities at various depths were used to calculate conditional probabilities for each of the parameters. The conditional probabilities predicted for various values of the critical parameters can be used with the measurements of flow and methane percentage at gob gas ventholes to optimize their performance.

Published by Elsevier Ltd.

1. Introduction

For gas control during longwall mining, drilling vertical gob gas ventholes (GGV) ahead of mining from the surface is a common technique in the US to capture methane emissions within the overlying fractured strata before it enters the work environment. Although the drilling practices of GGVs may change based on local conditions, most gob gas ventholes are drilled to within a short distance, 30–40 ft, of the coal bed being mined and cased with steel pipe. Commonly, the bottom section of the casing (generally about 200 ft) is slotted and placed adjacent to the expected gas production zone in the overburden strata. GGVs become productive as mining advances under the ventholes and the gas-bearing strata that surround the well fractures and establish preferential pathways for the released gas to flow towards the ventholes [1]. In order for GGVs to capture more methane and less mine air, the length of the slotted sections and their proximity to top of the coal bed should be designed based on the potential gas sources, their locations and the fracturing and displacements in the overburden that will create potential flow paths for the gas.

Palchik [2] reported that, based on the measurements in the Donetsk coal basin, the thickness of the fractured zone can vary up to 100 times the height of the mined coal seam depending on the size of the panel and the geology and geomechanical properties of the layers. Hasenfus et al. [3] divided the overlying strata into four main zones of specific properties: a gob, a highly fractured zone, a composite beam zone and a surface layer. Among these, gob and highly fractured zones are the prime interests in term of gob gas productivity since they have high permeabilities and form pathways for gas transport towards the ventholes or towards the mining environment, provided that there are gas emission sources within these intervals.

The characteristics of fracturing and the subsidence of overburden are revealed through predictive techniques and field studies [4,5]. Fawcett et al. [6] described a theoretical investigation into the zones of increased hydraulic conductivity caused by rock failure above a longwall panel. They correlated predicted failure heights with existing experimental values. Whittles et al. [7,8] conducted studies on the effects of different geotechnical factors on gas sources and gas flow paths for UK longwall operations. They studied how roof geology and its interactions

* Corresponding author. Tel.: +1 412 386 4008; fax: +1 412 386 6595.
E-mail address: cok6@cdc.gov (C. Özgen Karacan).

1365-1609/$ - see front matter Published by Elsevier Ltd.
doi:10.1016/j.ijrmms.2010.08.006

with boreholes may cause the deformation and closure of the boreholes drilled for methane control.

It is difficult to predict production performance of gob gas ventholes due to the involvement of multiple influential factors and due to the unknowns related to strata fracturing and gas emission intervals. Main factors and unknowns are drilling depths of the boreholes, size of the casing, vacuum generated by exhausters, atmospheric pressure conditions, location of the boreholes on the panels, strength and thickness of formations in the overburden. There are CFD (computational fluid dynamics) and reservoir simulation based models [9,10] but these models are complex and the outputs are only as good as the input data provided to them. The latter is a major constraint before a realistic output can be obtained from these models and predictive studies can be performed.

In order to come up with realistic but simpler solutions to GGV productivity and design issues, Palchik [11] proposed a mathematical model for estimation of productivity of gob gas ventholes associated with coal mining in the Torezko–Snezhnyanskya coal district. He established a relationship between methane emission from GGVs and the duration of well production using the Gaussian error distribution function and the Gaussian density function. However, he noted that in the mining area he studied, ~90% of total gob gas originated from the mined coal itself and the contribution from additional gas resources over the extracted seam was insignificant. Thus, this analytical approach may not represent situations where the gob gas generally originates from the fractured strata overlying the extracted seam.

Karacan [12] developed an artificial neural network (ANN) based model using field data to predict GGV production rates and methane concentrations for situations where most of the gas came from overlying strata and associated gas sources. Although this model was successful in addressing some of the GGV design issues and in establishing sensitivity studies, it treated the gas as a bulk quantity. It did not differentiate between different intervals that might be contributing to total flow to define the design and location of different slotted casing lengths. Also, Karacan [13] used multi-rate drawdown well test analyses techniques to evaluate the reservoir properties of fractured gob using rate and pressure data of GGVs. Although, this method is highly effective in reconciling gob parameters, it is insufficient to define where is gas is coming from due to representing the production interval as a single entity.

Despite the improvements in analytical and numerical modeling approaches, experience suggests that it is still difficult to properly design the GGVs and to accurately predict their productions. It is not uncommon that the predictions may under- or overpredict the actual values by a factor of one or two. One of the key causes of these erroneous predictions is the difficulty in understanding the quantity and location of the gas sources in the overlying strata.

In this study, a probabilistic approach to determine the depth-displacement, depth-flow percentage, depth-formation and depth-gas content is proposed using bivariate normal distributions. Conditional probabilities are calculated for fixed values of different variables with respect to height from coal seam and depth from surface and used to understand the flow and strata behavior and to design casing lengths and their setting depths accordingly to optimize GGV performance.

2. Overlying formation in Northern Appalachian coal-mining basin

This study was performed using the data obtained from the coal mines located in Southwestern Pennsylvania and Northern West Virginia of the Northern Appalachian Basin. Thus, a brief description of formations that belong to this area and forming the fractured zone during longwall mining is necessary. A detailed description of the

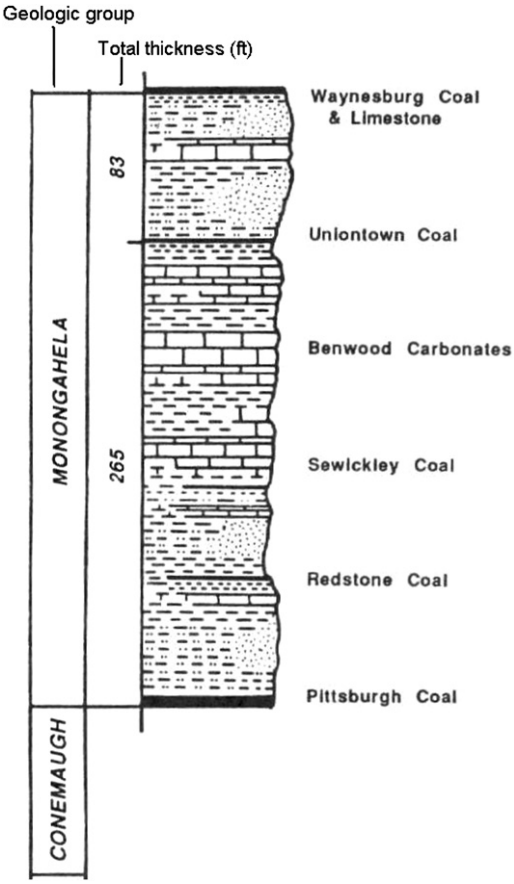

Fig. 1. General stratigraphic log of the formation overlying Pittsburgh seam. This interval constitutes the caved and fractured zones of gob.

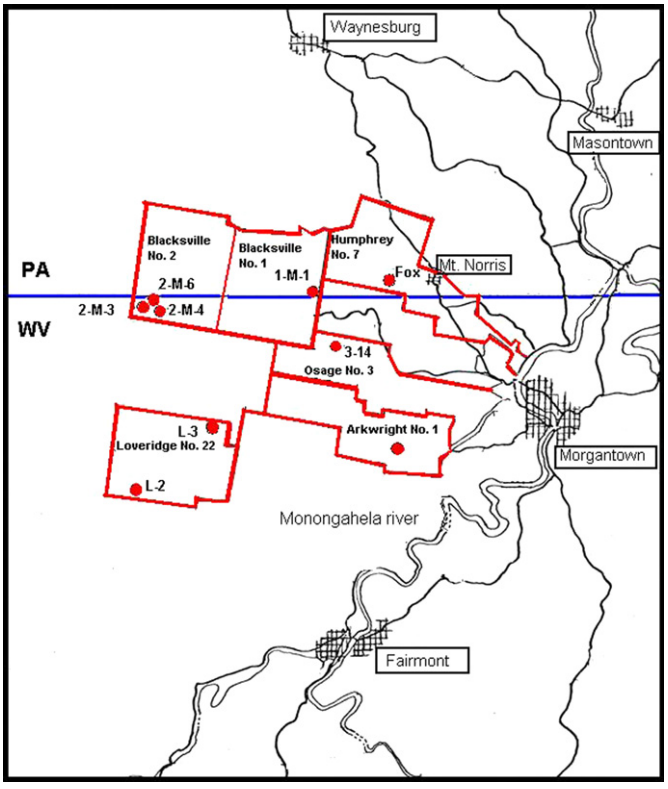

Fig. 2. Names and locations of the tested boreholes and the associated mine properties.

strata layers, the properties of coal-measure formations overlying the Pittsburgh coal seam and their reservoir characteristics are given elsewhere [5,14]. However, for completeness of this paper and the work presented, a brief overview is given in this paper too.

From coal mining and gas control perspectives, the Monongahela Group in Northern Appalachian Basin is the most important. It is located within the Pennsylvanian age sediments and encompasses the stratigraphy from the base of the Pittsburgh coal bed to the base of the Waynesburg coal bed, extending to a thickness 270–400 ft (Fig. 1).

The general coal measures in the Monongahela Group in Greene County shown in Fig. 1, and their thicknesses from top to bottom of the group, can be listed as: Waynesburg main coal bed (5.9 ft), clay (2.9 ft), sandstone (19.7 ft), limestone (4.9 ft), sandstone and shale (60 ft), Uniontown coal bed (1–3 ft), Upper Great limestone-Benwood (17.7 ft), Sewickley sandstone and shale (60 ft), Lower Great limestone-Benwood (55 ft), sandy shale (12.2 m), Sewickley coal bed (1–6 ft), sandstone (9.8 ft), the Fishpot limestone (17.7 ft), sandstone and shale (25 ft), Redstone coal bed (1–4 ft), limestone (9.8 ft), Pittsburgh upper sandstone (39.4 ft), shale (0 to 9.8 ft) and Pittsburgh coal bed (4.9–12.1 ft).

3. Data profiles used in probabilistic model development

3.1. Borehole tests for data compilation and flow characterization

The flow entry tests, strata separation determinations and strata identifications were performed during a study reported in [15]. That study was performed in coal mines of Northern West Virginia, which are known for their gassy nature and use gob gas ventholes to control underground emissions by capturing the strata gas. During the course of this project 8 GGVs were drilled over different coal mines working in the Pittsburgh coal seam. Fig. 2 shows the ventholes and the associated mine properties where that they were drilled.

Table 1 gives the summary of the reported completion details of the ventholes, their initial gas production start, the displacement and flow profiling measurements with respect to the face location. This table also gives the general observations reported and measurements taken during flow profile and displacement measurements, whose experimental details are given in the following sections. This table shows that the general observations of strata separation locations are in general agreement with the predictions reported in various publications based on the strength of rock layers and their density and gamma ray log readings [2,5,16].

In this paper, the data from flow, strata separation and core identification measurements of all ventholes were digitized and compiled to be presented in graphical form. These graphs of measurements are given in the following sections. These data are also used as the raw data for bivariate normal distribution modeling that is presented in detail later in this paper.

3.1.1. Flow entry profiles

Gas flow entry locations in gob gas ventholes were obtained with a pulse-type logger. This system contained a cylinder in which a mixture of Kyrpton-85 and nitrogen was stored at an

Table 1
Summary (compiled from [15]) of the completion details of the ventholes as well as initial gas production start, displacement and flow profiling measurements with respect to the face location. The lower part of this table also gives the general observations reported during flow and displacement (subsidence) profiling.

Venthole name	Venthole completion	Start of gas production	Subsidence survey[a]	Flow profile survey[a]
1-M-1	?	0	+50/+575	+310
Fox	Drilled to 18-ft to Pittsburgh seam; 310-ft slotted casing	+20	+350	+10/+350
L-2	Drilled to 18-ft to Pittsburgh seam; 334-ft slotted casing	0	+195	+195
3–14	Drilled to 20-ft to Pittsburgh seam; slotted casing to 20-ft above Sewickley seam	+50	+110	?
2-M-3	Drilled to 18-ft to Pittsburgh seam; 328-ft slotted casing	+10	+270	+100
2-M-4	Drilled to 90-ft to Pittsburgh seam; Bottom 29-ft open hole	+70	+145	+130
L-3	Drilled to 99-ft to Pittsburgh seam; Bottom 34.5-ft open hole	0	?	?
2-M-6	Drilled to 82-ft to Pittsburgh seam; 238-ft slotted casing; Bottom 20-ft open hole	+58	+58	+80

General observations during subsidence and flow profile measurements

Venthole name	Subsidence test	Flow profile test
1-M-1	Major strata separation at ~125-ft above Pittsburgh seam close to top of Sewickley sandstone. Underlying interval had additional separations	70% of the flow entered the hole within 120-ft above Pittsburgh seam. No flow observed within 80-ft of the coal bed
Fox	Strata separations above ~280-ft of the mine. Major separation at ~150 above the mine	In the first test, little flow was observed. In the second test majority of flow entered near Sewickley sandstone and Uniontown limestone
L-2	Separations were measured ~270 ft above the mine. Large displacements were located just above Sewickley coal	No flow near the mine with an increase in flow ~70 ft above the mine near a limestone. Major flow entry occurred from a 10-ft sandy shale
3–14	Two strata separations of ~0.8-ft at 100 and 235 ft above the Pittsburgh coal seam	Short lived production to determine the flow entry profile
2-M-3	Strata movements near Waynesburg coal at 320 ft above the mine. Majority of separations occurred below ~109-ft above Pittsburgh coal	No flow existed near the mine
2-M-4	The displacement was found nearly linear with depth above Sewickley sandstone. At least 1.5 ft cumulative strata separation 140-ft above the mine near Sewickley sandstone	All flow entered the hole at the top of Sewickley sandstone, 110-ft above the mine
L-3	Strata appeared to be broken over a zone of reaching ~225-ft above the Pittsburgh seam	?
2-M-6	Separations of 0.2-ft occurred near Waynesburg coal and Sewickley sandstone	~85% of flow entered the hole in a 100-ft interval from a gray shale formation to the Sewickley sandstone

[a] "?": Unreported values or conditions; "+": the distance of the face past the borehole.

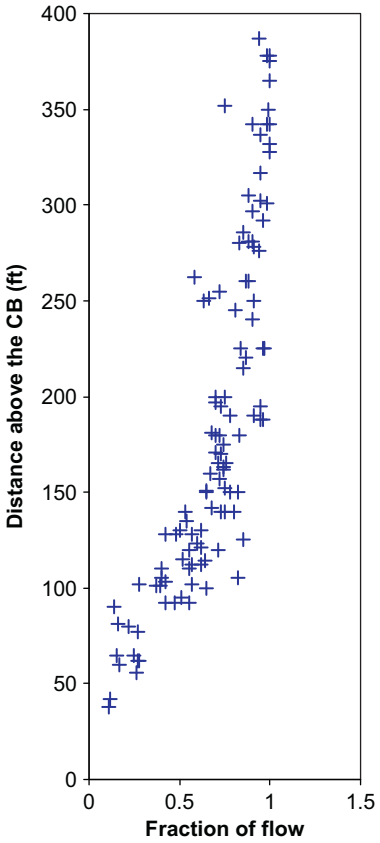

Fig. 3. Combined flow profiles obtained from all ventholes.

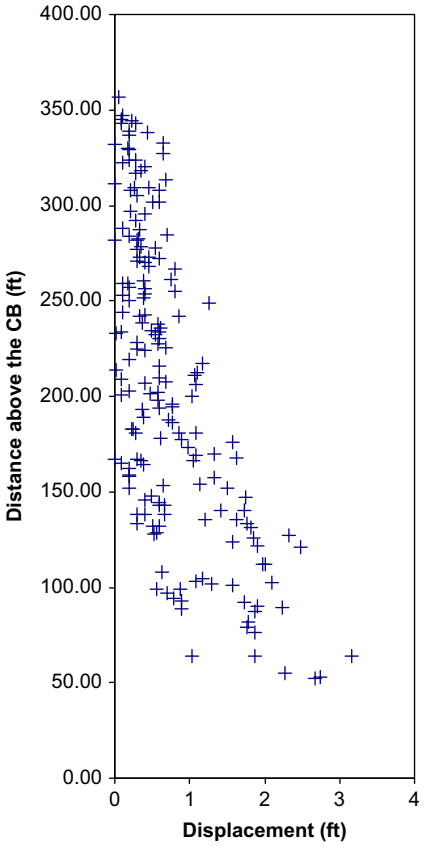

Fig. 4. Combined strata separations (exclusive of surface subsidence) obtained from all ventholes.

initial pressure of 800 psi. This amount of gas was enough approximately for 250 pulses.

This device was suspended in the borehole from the gamma-ray tool with a four-conductor armored cable that permitted activation of a solenoid valve to release the krypton gas mixture as pulses. The downhole position accuracy of this device was found to be ± 0.1 ft [15].

A pulse of ^{85}Kr tagged nitrogen was released and the formation gas which carried the tracer gas to the gamma-ray tool and its arrival time were recorded. The system basically recorded the transit time of a pulse of radioactive gas to travel a known interval while being carried in the stream of produced gas. The recorder was driven at a preselected constant rate and also recorded the radiation anomaly created by the passing of the krypton. The velocities were then determined with the known time and distance [15], from which flow rates and flow percentages coming from each flow entry point in the borehole could be calculated.

Fig. 3 shows the results of the combined flow profile, which has been constructed by digitizing the data from measurements of all ventholes. In order to be able to show all flow rates in the same scale, the data were normalized and are shown as fractions of flow. This figure shows that only a minor percentage of flow enters the ventholes within 50 ft of the mined coal bed. A significant increase in the flow entry occurs at approximately 100 ft above the mined coal seam, where Sewickley sandstone is located. The percentage of flow originating at this interval varies between 50% and 70% of the total flow at different ventholes. As it is shown in Fig. 4 and discussed in the next section, this interval corresponds to where major displacements or strata separations occur in the overburden. However, it should be noted that this interval may not necessarily correspond to the source of the gas, but the location of the major flow pathways. Another observation from Fig. 3 in conjunction with the face locations at the time of flow entry measurements is that the position of the face does not influence the flow profile drastically. Finally, Fig. 3 shows that almost all flow enters the venthole below at about 250 ft from the mined coal bed.

3.1.2. *Displacement (strata separation) profiles during subsidence*

In order to locate the displacements and to measure the strata separations during subsidence, radioactive tagged shaped charges were used in the gob gas ventholes. These charges were used in the ventholes to implant radioactive markers into the formations to measure the subsidence and the strata separation during mining.

^{60}Cobalt was used as the radioactive material in the charges. The charges had the radioactive kernels glued to the liner in two separate configurations. Half of the charges contained radioactive kernels located inside the cone, at 1/3 of the distance from the

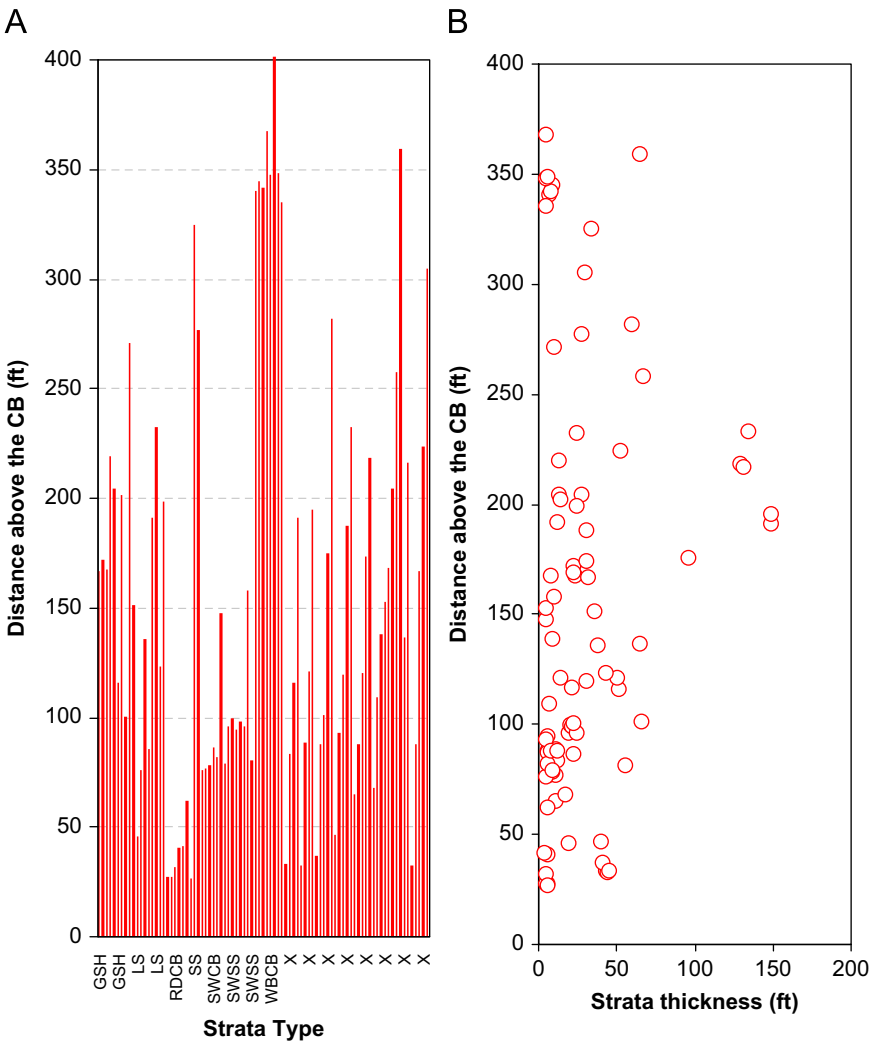

Fig. 5. Strata type (A) and their thicknesses (B), with respect to distance from Pittsburgh coal bed, measured in the ventholes (GSH: gray shale; LS: limestone; SS: sandstone; RDCB: redstone coal bed; SWCB: Sewickley coal bed; SWSS: Sewickley sandstone; WBCB: Waynesburg coal bed; X: mostly shales of various kind).

apex to the base. The others contained kernels located at 2/3 of the apex–base distance [15].

The charges were fired through tubing. It was found that the markers actually did not contaminate the tubing for subsequent measurements and were implanted into the formation with a success rate of nearly 100% to mark the formations. This technique ensured correct measurement of the formation movements and the locations of strata separations with gamma ray logging [15].

Fig. 4 shows the results of the combined displacement profiles that give the amounts of strata separations, which have been constructed from measurements of all ventholes. The values shown in this figure are exclusive of any surface subsidence since the measurements were made using the well head as a datum and the displacements calculated are subtractions of strata subsidence and well head subsidence.

Fig. 4 shows that vertical displacements due to strata separations can be effective as high as 300–350 ft from the Pittsburgh coal seam. The magnitude of strata separations between this and down to almost 200–250 ft above of the Pittsburgh seam are generally less than 1 ft, mostly around 0.5 ft. The displacement trend in this interval is almost linear and not a function of depth. However, at ~200 ft above the Pittsburgh coal bed and below, the separations starts to depart from low displacement values and major strata separations in the order of 2 ft can be measured. These high separations are mostly 100 ft above the mine where Sewickley sandstone occurs. This observation and the displacement measurements are in line with the flow entry measurements discussed in the previous section. Displacement trend at and below 200 ft also follows a nearly linear trend with a ~45° relationship with depth.

3.1.3. Strata type and thickness profiles

Strata identifications and their thicknesses were evaluated from core logs and electric logs. As discussed in Section 2, this region hosts shales, three major coal seams, and limestone and sandstone units. The thicknesses of almost all formations change based on location, which is a characteristic of depositional environments that has been created in lacustrine and swamp conditions [14].

Fig. 5a and b shows main strata types (A) and their thicknesses (B), with respect to distance from Pittsburgh coal bed, measured in the ventholes. In these graphs, the pictorial information given in [15] was digitized to obtain the depth and thickness information and plotted for quantitative information. These figures show that Waynesburg coal bed is around ~350 ft from the Pittsburgh coal bed and its thickness is ~5 ft. At the 200 ft interval, gray shale is dominant with a varying thickness of 20–30 ft. Sewickley coal bed and Sewickley sandstone, on the other hand, are between 75 and 100 ft from the Pittsburgh seam with thicknesses of 5–6 and ~25 ft, respectively. This zone is identified as the interval where most of the displacement occurs and where most of the gas enters the ventholes. The formations, whose thicknesses may be up to

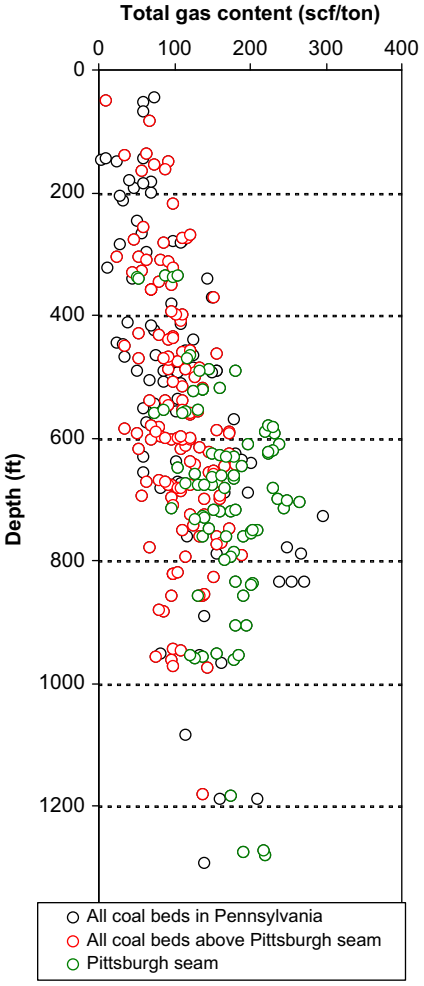

Fig. 6. Gas content-depth relationship of all coal beds in Pennsylvania, Pittsburgh seam and overlying seams.

100–150 ft, are the limestone and shale units that are located ~150–225 ft from the Pittsburgh seam. Formation thickness information was further divided by the representative Young's modulus data of the formations to compound them with the formation-type information.

3.2. Gas content profiles

There are two major sources for the gas produced from GGVs. One of them is the mined coal bed itself, and the other is the overlying strata and its potential gas sources. In the latter case, coal beds with enough gas potential are the most likely sources of gas. This suggests that if the gas content of the coal bed that is source of the gob gas is high, the gas emissions to be captured by GGVs can be high also.

In this paper, the gas contents of all coal beds given in [17] in Pennsylvania were compiled in a database and all the coal beds above the Pittsburgh seam and including the Pittsburgh seam itself were classified. Coal seam gas content and depth relationship for these classes were plotted in Fig. 6. The majority of the data plotted in Fig. 6 was obtained from high-volatile-bituminous-A type coals, some from medium volatile coals, and the gas content-depth relationship generally shows an increasing trend

Table 2
Mean (μ) and standard deviation (σ) of each variable and the correlation coefficients (ρ) between variable pairs used in calculating joint probability distributions.

Data pairs		Correlation
Flow (fraction)	Distance from coal bed (ft)	
$\mu=0.699$	$\mu=196.56$	$\rho=0.906$
$\sigma=0.244$	$\sigma=100.395$	
Displacement (ft)	Distance from coal bed (ft)	
$\mu=0.746$	$\mu=205.22$	$\rho=-0.676$
$\sigma=0.638$	$\sigma=79.367$	
Total gas (scf/ton)	Overburden (ft)	
$\mu=122.700$	$\mu=588.837$	$\rho=0.558$
$\sigma=54.766$	$\sigma=233.564$	
Formation thick/E (ft/GPa)	Distance from coal bed (ft)	
$\mu=7.484$	$\mu=154.351$	$\rho=0.117$
$\sigma=7.921$	$\sigma=98.254$	

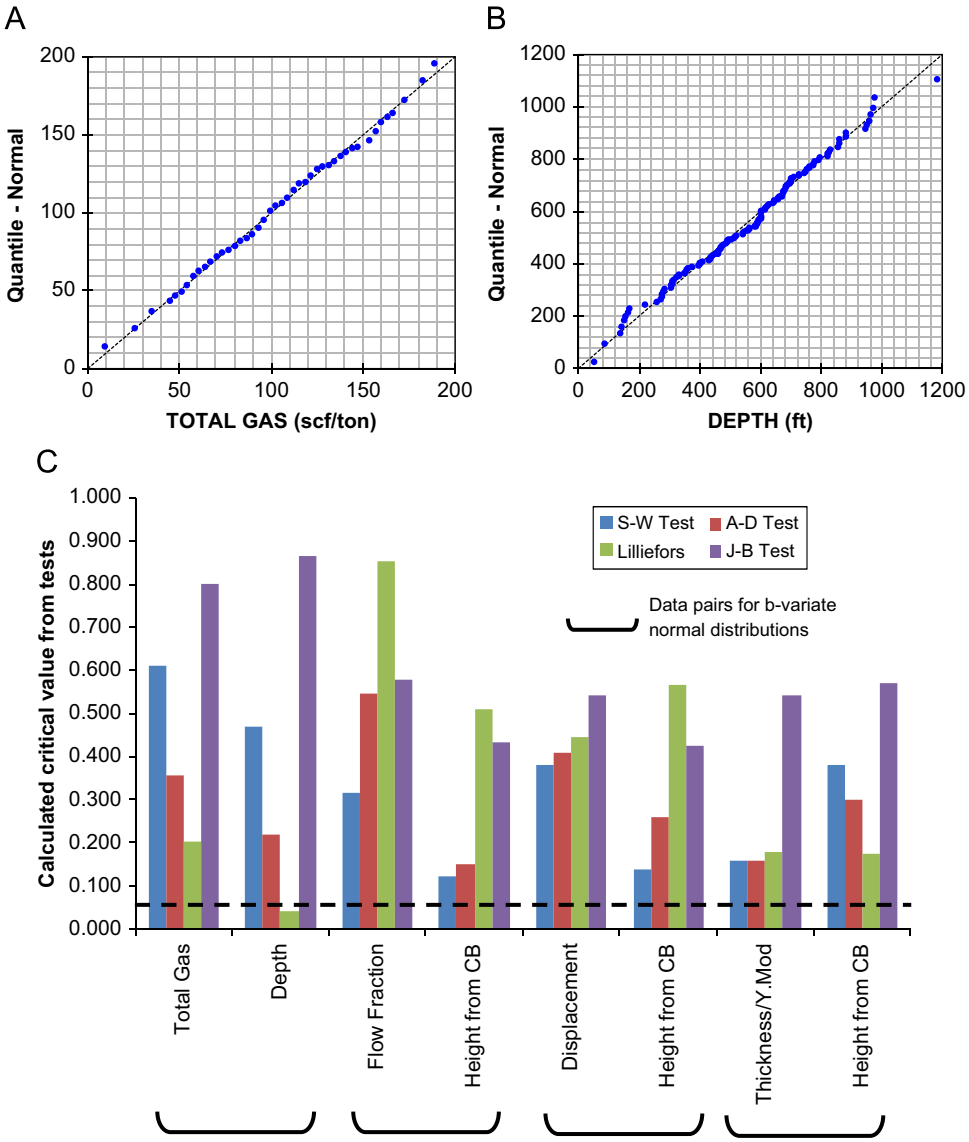

Fig. 7. Q–Q plots for flow gas content (A) and depth data (B) obtained from all GGVs listed in Table 1. Figure C gives the critical values calculated for all data sets using four normality tests (Shapiro–Wilk, Anderson–Darling, Lilliefors and Jarque–Bera) to see if the data are from a normal distribution (null hypothesis) for a significance level 5%, shown by the dashed line.

with depth. However, it should be also noted that gas contents show significant variations even at the same depth.

In this work, based on the two premises for the source of gob gas, gas content-depth data of Pittsburgh coal and the gas content-depth data of all other coal beds overlying the Pittsburgh seam were used in modeling the source of the gas and its gas content.

4. Probabilistic modeling approach

4.1. Bivariate normal distribution—probabilities of multivariable events

It is generally recognized that complex geological and hydrological events always appear to be multivariate events. Events of this nature can best be characterized by a few correlated random variables and by their joint probabilistic properties, rather than single-variable analyses as these can only provide limited assessment of these events [18].

Gas emissions from gob and methane production using gob gas ventholes can be characterized as an event with multiple episodic phenomena, which is controlled by multiple variables, such as distance from mining environment, gas content of strata, strata separations, etc. A thorough understanding of the multivariate nature of gob gas emissions and capture requires analysis of the joint probability of two or more correlated random variables. Such an analysis characterizes the gob formation process and better designs the gob gas venthole completion parameters, such as the depth and length of the slotted casing.

The normal distribution is the most commonly used distribution to model univariate data from a population or from an experiment [19]. In order to extend this concept to the bivariate case, let us assume we have two variables, X and Y, each of which is individually normally distributed. Each of these variables can be transformed into a standard normal random variable, which can be called as Z_1 and Z_2. These variables can be shown by the relationships:

$$Z_1 = \frac{X-\mu_X}{\sigma_X} \tag{1}$$

$$Z_2 = \frac{Y-\mu_Y}{\sigma_Y} \tag{2}$$

where μ_X and μ_Y are the mean values of X and Y, and σ_X and σ_X are

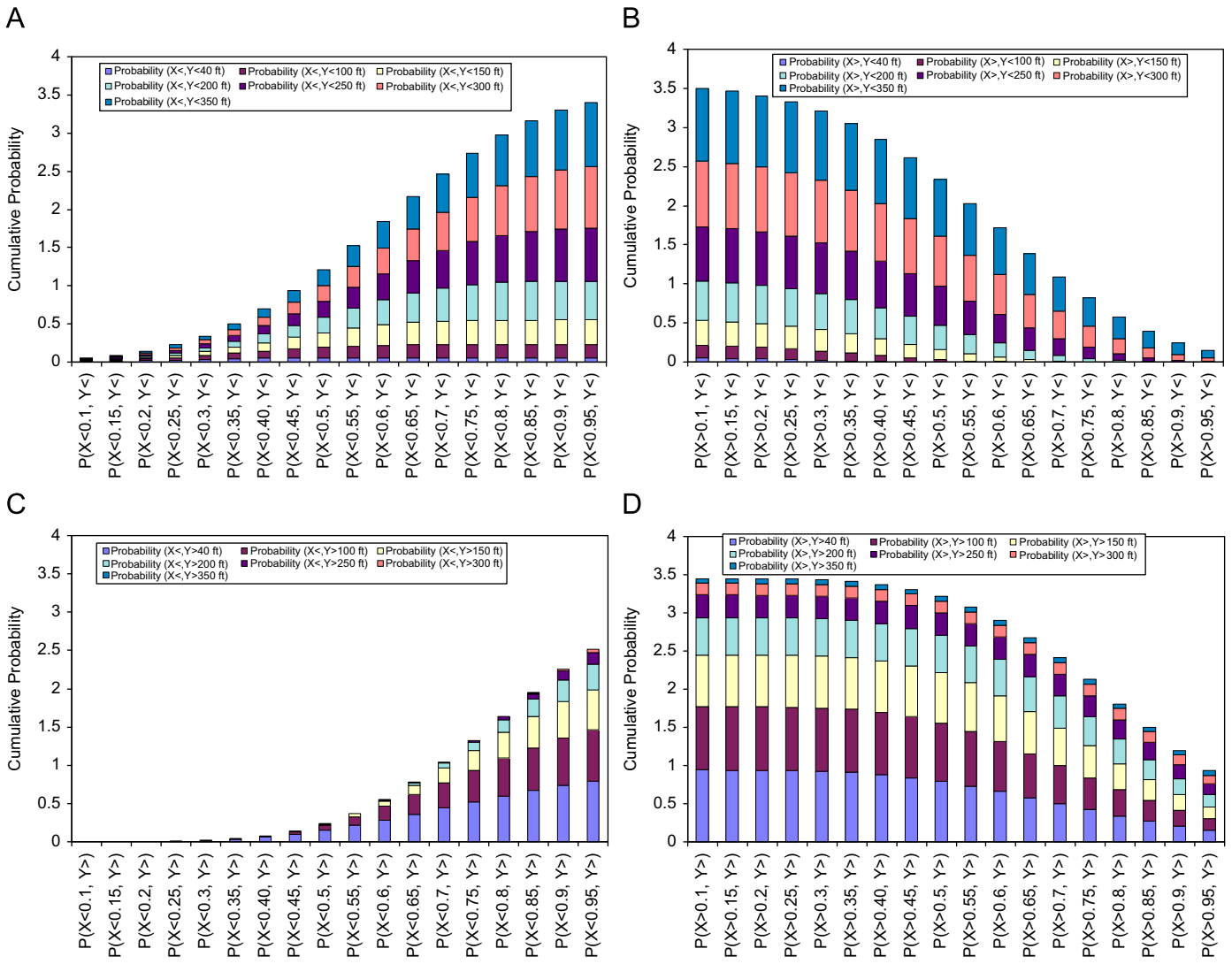

Fig. 8. Conditional probabilities: (a) $P(X_1 \le a, X_2 \le b)$, (b) $P(Z_1 > a, Z_2 \le b)$, (c) $P(Z_1 \le a, Z_2 > b)$ and (d) $P(Z_1 > a, Z_2 > b)$, calculated for flow and distance-from-coal bed data using bivariate normal distribution.

the standard deviations of X and Y. The standard normal bivariate probability density function is then:

$$f(Z_1,Z_2,\rho)=\frac{1}{2\pi\sqrt{1-\rho^2}}\exp\left[-\frac{1}{2}\left(\frac{Z_1^2-2\rho Z_1Z_2+Z_2^2}{1-\rho^2}\right)\right] \quad (3)$$

where ρ is the correlation between the two variables.

All of the tail or conditional probabilities that can be calculated using the bivariate probability density function (3) can be given as [19]

$$P(X_1\le a,X_2\le b)=P\left(Z_1\le\frac{a-\mu_1}{\sigma_1},Z_2\le\frac{b-\mu_2}{\sigma_2}\right) \quad (4)$$

$$P(Z_1\le a,Z_2>b)=\Psi(a)-P(Z_1\le a,Z_2\le b) \quad (5)$$

$$P(Z_1>a,Z_2\le b)=\Psi(b)-P(Z_1\le a,Z_2\le b) \quad (6)$$

$$P(Z_1>a,Z_2>b)=1-\Psi(a)-\Psi(b)+P(Z_1\le a,Z_2\le b) \quad (7)$$

where Ψ is the standard normal distribution function and P is the probability.

4.2. Normality check for the data sets

In this study, six random data sets were complied from the field experiments and used for calculating their joint probabilities using bivariate normal distributions to characterize the flow and displacement intervals. These data sets are flow fraction, displacement, strata thickness divided by Young's modulus, distance from the mined coal bed, gas content of the strata and overburden depth. The random data used in bivariate normal distribution calculations for joint probabilities were flow fraction – distance from the coal bed, displacement – distance from the

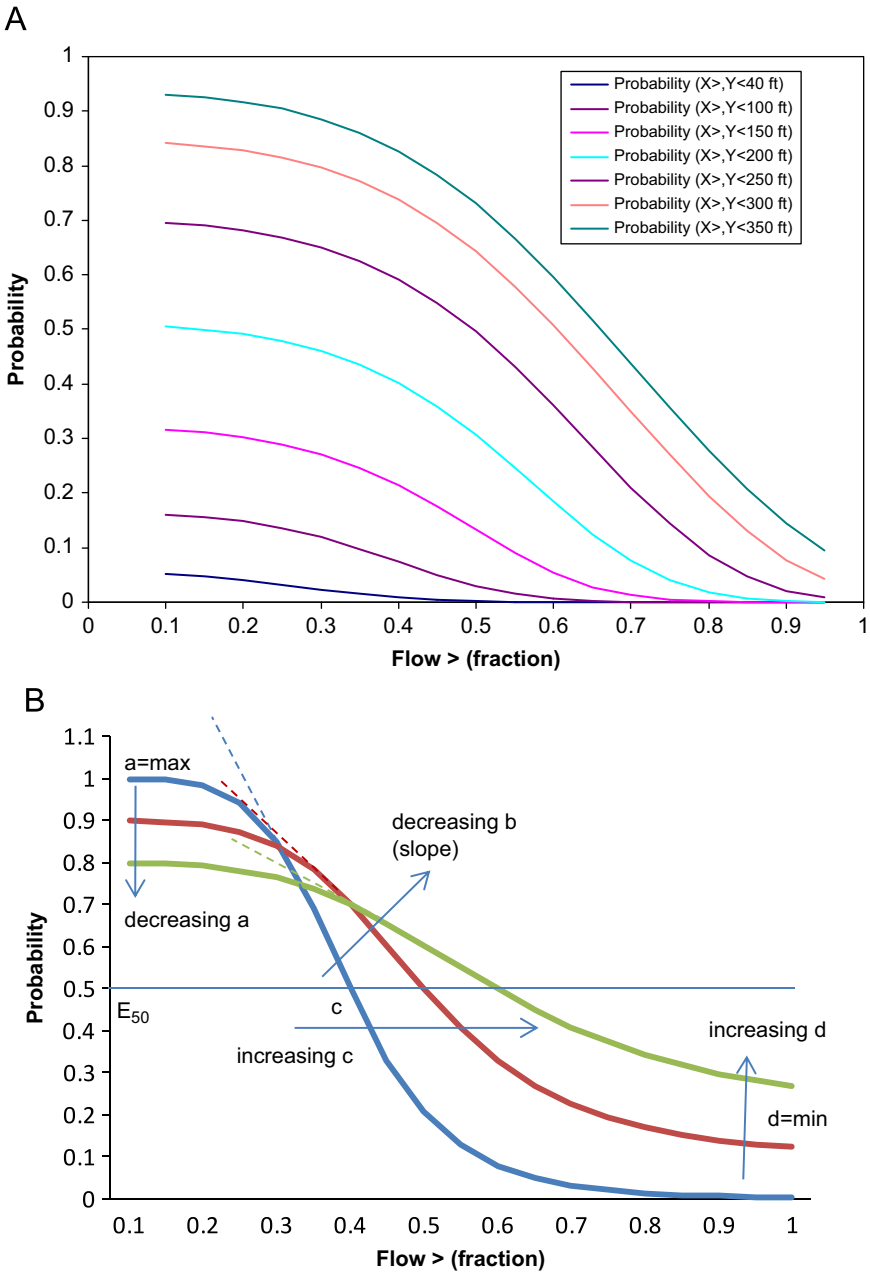

Fig. 9. (a) Conditional probabilities calculated for different flow and distance-from-coal bed cases for the $P(Z_1>,Z_2\le)$ region shown in Fig. 8b. (b) Locations of parameters of logistic function given in Eq. (10) and how the change in these parameters can affect the shape of the function.

coal bed, strata thickness divided by Young's modulus – distance from the coal bed, and gas content – overburden depth pairs.

In order to be able to use the above pairs in bivariate normal distribution modeling, the univariate data sets should be checked whether they are actually from a normal population. For this purpose, the data (observed quantiles—$X(j)$) was first ordered and the cumulative probability level of each observed quantile, which is approximately equal to [19]

$$\frac{j-0.5}{n} \tag{8}$$

was calculated. In Eq. (8), n is the number of observations. For these cumulative probabilities, standard normal quantiles were then calculated using

$$\mu+\sigma\sqrt{2}erf^{-1}(2p-1) \tag{9}$$

where μ is the mean, σ is the standard deviation, erf is the error function and P is the cumulative probability level.

Fig. 7a and b shows the quantile plots (Q–Q) for total gas content of coal seams (Fig. 7a) and depth-from-surface data (Fig. 7b), as an example of the normality tests applied to all data sets used in this work. If the data are from a normal population, the Q–Q plots should be approximately linear. Fig. 7a and b shows that the Q–Q plots are linearly related, suggesting normal distribution of these two data sets.

In order to further make sure that the data are from normal distributions, four different normality tests, namely Shapiro–Wilk, Anderson–Darling, Lilliefors and Jarque–Bera tests, were also performed on each of the data sets [20]. These tests assume as a "null hypothesis" that the data are from a normal distribution and compare calculated critical values with the selected significance level (5% in this study). In order for the null hypothesis to be accepted, calculated critical values should be greater than the significance level. The calculated critical values for each of the data sets for each test are shown graphically in Fig. 7c. This figure shows that calculated critical values are all (except the depth data in Lilliefors test) are greater than 0.05 and thus the data sets are presenting the properties of a normal distribution. Therefore, the bivariate normal distributions could be used in calculating the joint probabilities for the data set pairs given above to characterize the flow amount and displacements in longwall gobs.

Table 3
Parameters of the logistic equation (Eq. (10)) that were determined to calculate conditional probabilities of different variables in the $P(Z_1>, Z_2\leq)$ range.

Distance from CB (ft)	R^2	d	a	c	b
Displacement > ; distance from CB ≤					
40	0.9986	3.8389E−12	0.0185	1.7813	6.5169
100	0.9979	1.9142E−11	0.0897	1.5026	5.4938
150	0.9973	5.2739E−11	0.2333	1.2887	4.7205
200	0.9966	1.0862E−10	0.4441	1.1075	4.0799
250	0.9959	1.7154E−10	0.6439	0.9757	3.6195
300	0.9953	2.1844E−10	0.7606	0.9020	3.3551
350	0.9949	2.3997E−10	0.8003	0.8748	3.2504
Flow fraction > ; distance from CB ≤					
40	0.9964	1.0418E−11	0.0508	0.2832	4.8374
100	0.9920	5.2001E−11	0.1548	0.3841	5.5736
150	0.9952	1.6266E−10	0.3027	0.4672	6.0580
200	0.9942	4.3447E−10	0.4847	0.5409	6.2502
250	0.9932	9.9653E−10	0.6693	0.6030	6.0522
300	0.9937	6.4490E−12	0.8154	0.6483	5.5533
350	0.9956	4.7585E−12	0.9068	0.6763	5.0755
Strata thickness/Young M > ; distance from CB ≤					
40	0.9964	5.20E−11	0.0866	8.623	2.8872
100	0.9920	1.30E−10	0.2097	8.8791	2.9193
150	0.9952	2.24E−10	0.3543	9.0757	2.9439
200	0.9942	3.24E−10	0.5022	9.2433	2.9647
250	0.9932	4.09E−10	0.6244	9.3789	2.9812
300	0.9937	4.64E−10	0.7011	9.4726	2.9921
350	0.9956	4.92E−10	0.7383	9.5264	2.998
Gas content > ; overburden ≤					
Overburden (ft)	**R^2**	**d**	**a**	**c**	**b**
100	0.9984	2.66E−12	0.0145	57.5716	3.2447
300	0.9957	3.45E−11	0.096	71.9543	3.2503
500	0.9945	1.44E−10	0.3238	92.7746	3.8831
700	0.9962	2.45E−10	0.6424	108.3495	4.4266
900	0.9962	3.97E−10	0.8625	117.2951	4.4184
1100	0.9960	4.90E−10	0.9389	121.1653	4.3581
1300	0.9961	5.10E−10	0.9519	121.9739	4.3293

4.3. Calculating joint probabilities using bivariate normal distributions

Joint probabilities of four different variable pairs were calculated for all tail probabilities of a bivariate normal distribution using Eqs. (3)–(7) and the means, standard deviations and the correlations given in Table 2. In calculating the probabilities, flow,

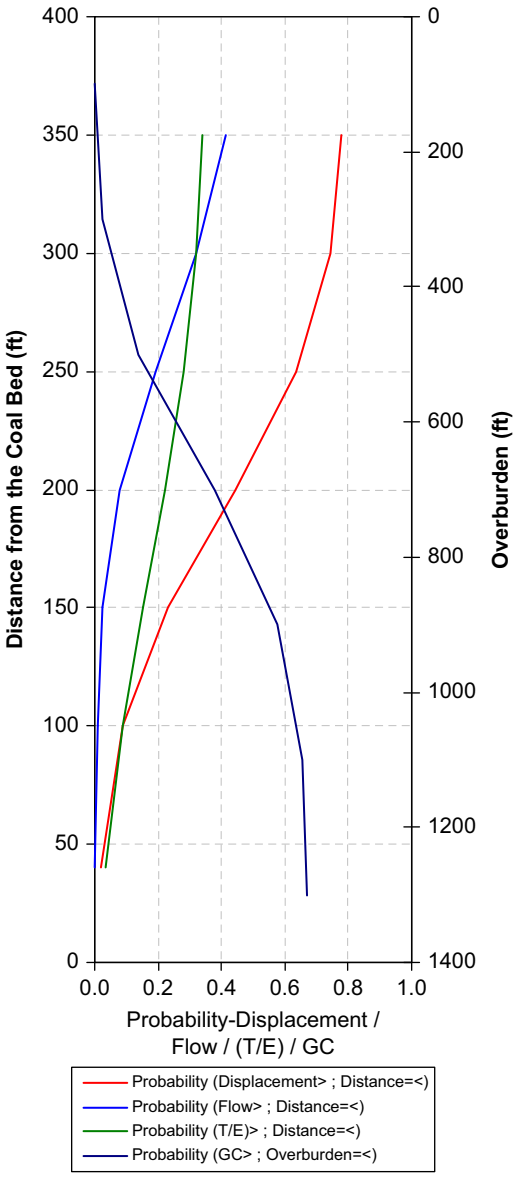

Fig. 10. Conditional probabilities for displacement (0.3 ft), flow (70%), T/E (10 ft/GPa) and gas content (100 scf/ton) obtained as a function of distance from the coalbed and overburden for $P(Z_1>, Z_2\leq)$ range.

displacement, gas content and thickness data were selected as variable X term and distance variables were selected as Y term in Eqs. (1) and (2), respectively. Also, joint probabilities were calculated for various X and Y values so that a distribution of conditional probabilities could be established. The results of such a calculation for flow and distance-from-coal bed pair are given, as an example, in Fig. 8 for all calculated conditional probabilities. In this calculation, a range of flow fractions between 0.1 and 0.95 and a range of distances from 40 to 350 ft were used (Fig. 8). A similar approach was used for the other data pairs.

Although calculating conditional probabilities for all tails using different X and Y values and presenting the results as in Fig. 8 shows the joint probabilistic behavior of two variables and how they may characterize an event, the predictions of conditional probabilities are limited to the actual values used in calculations. In order to generalize the joint probabilistic behavior of each of the data pairs, four-parameter logistic equations were fitted to the calculated probabilities to create functional relationships. A four-parameter logistic equation is given in Eq. (10), and example data to which this equation is fitted is shown in Fig. 9a, which shows the flow versus conditional probability plot drawn using the data from Fig. 8b:

$$y = d + \frac{(a-d)}{1+(x/c)^b} = \min + \frac{(\max-\min)}{1+(x/E_{50})^{slope}} \quad (10)$$

The four-parameter logistic equation shown in Eq. (10) is one of the basic sigmoid functions that are used for various applications in biology and biochemistry such as growth rate and dose–response studies [21]. The nonlinear nature of this function makes it flexible to model data that show an "S" shape character. In Eq. (10), a, b, c, d are the maximum value (a) and minimum value (d) at asymptotes, slope at the hill of the line (b) and value of dependent variable at 50% value of independent variable (c) [21]. These parameters are shown schematically in Fig. 9.

Table 3 gives the parameters of the logistic equations fitted to different variables to calculate their conditional probabilities in the $P(Z_1 >, Z_2 \leq)$ range. As this table shows, the logistic equation was able to fit the data similar to shown in Fig. 9 with regression coefficients of more than 0.99. Similar equation fits to variables were performed to calculate their conditional probabilities in other regions of probabilities given in Eqs. (4)–(7). It was seen that all tail probabilities can be represented with sufficient accuracy using logistic equations and that estimating the probabilities using logistic functions can help interpolate the probabilities and make calculation of probabilities more flexible.

5. Results and discussion—application of the technique

The bivariate normal distributions and the technique shown to calculate joint and conditional probabilities can be used to determine where a certain amount of flow might be inflowing into the borehole during longwall mining and where a certain

Table 4
Conditional probabilities for strata separations more than 0.3 ft and less than 0.8 ft, and fractions of total flow more than 0.5 and less than 0.9 for all regions of the bivariate normal distribution as a function of distance from the coal bed.

Displacement (ft) >	Distance CB (ft) ≤	Probability	Flow >	Distance CB (ft) ≤	Probability
0.3	40	0.018	0.5	40	0.001
	100	0.090		100	0.008
	150	0.233		150	0.024
	200	0.442		200	0.081
	250	0.635		250	0.193
	300	0.742		300	0.322
	350	0.776		350	0.414
Displacement (ft) ≤	Distance CB (ft) ≤	Probability	Flow ≤	Distance CB (ft) ≤	Probability
0.8	40	0.000	0.9	40	0.060
	100	0.005		100	0.171
	150	0.033		150	0.329
	200	0.126		200	0.516
	250	0.286		250	0.681
	300	0.432		300	0.759
	350	0.512		350	0.773
Displacement (ft) >	Distance CB (ft) >	Probability	Flow >	Distance CB (ft) >	Probability
0.3	40	0.765	0.5	40	0.490
	100	0.694		100	0.499
	150	0.548		150	0.491
	200	0.335		200	0.425
	250	0.140		250	0.288
	300	0.035		300	0.151
	350	0.005		350	0.063
Displacement (ft)	Distance CB (ft) >	Probability	Flow ≤	Distance CB (ft) >	Probability
0.8	40	0.547	0.9	40	0.727
	100	0.545		100	0.625
	150	0.513		150	0.472
	200	0.411		200	0.285
	250	0.251		250	0.113
	300	0.110		300	0.023
	350	0.034		350	0.002

amount of strata separation might happen. The probabilistic results given for strata thickness and gas content estimations can also be used in relation to flow and displacement probabilities. The ultimate benefit of applying the presented techniques is the ability to specify gob gas venthole parameters, particularly the location of the borehole and length of the slotted casing.

Fig. 10 shows the calculated conditional probabilities for the occurrence of more than 0.3 ft strata separation and more than 70% of flow inflowing to the borehole. This figure shows that the probability of more than 0.3 ft strata separation occurring below 350 ft during mining decreases from 0.8 to 0.05 below 40 ft from the top of the coal bed. Similarly, the probability of more than 70% of the total gas flow entering into the borehole below 350 ft decreases from 0.45 to 0 below 40 ft. These data can be used in conjunction with strata thickness/Young's modulus ratio and gas content data. For example, the probability of overlying strata having more than 100 scf/ton gas increases to 0.7 at 900-ft overburden depth. The probability of finding this much gas at depths shallower than 900 ft is less than 0.7.

This data or the conditional probabilities obtained for different values of the variables can be used to design the GGV slotted casing lengths and to establish the depth at which they should be located. According to the example data presented in Fig. 10, if the casing is able to withstand the strains originating from a 0.3 ft strata separation, then it is safe to use it below 350 ft to the coal bed since the probability of more than 0.3-ft separations is decreasing below that distance. At this interval, the probability of this casing having more than 70% of the flow, however, is only 0.4 or less. For different strata-separations and flow capture goals, conditional probabilities can be calculated using different values for optimum design.

All tail probabilities for strata separation and flow can also be calculated to obtain detailed information about the probabilities of occurrence of separations and flow capture within a range of values. In Table 4, the conditional probabilities for strata separations more than 0.3 ft and less than 0.8 ft, and the fractions of total flow as 0.5 and 0.9 are presented for all regions of the bivariate normal distribution as a function of distance from the coal bed. The data are also given in graphical form in Fig. 11a and b.

Fig. 11a shows that the probability of a displacement or strata separation, more than 0.3 ft, is 0.8 at a distance less than 350 ft from the coal bed. The probability of having the same amount of strata separation starting from the coal bed is symmetrical and increases with distance. The intersection of these two curves (dotted red and dotted blue) gives the probability (0.4) and distance (~180 ft in this case) where at least 0.3 ft separation occurs in the overlying strata. The solid lines give the conditional

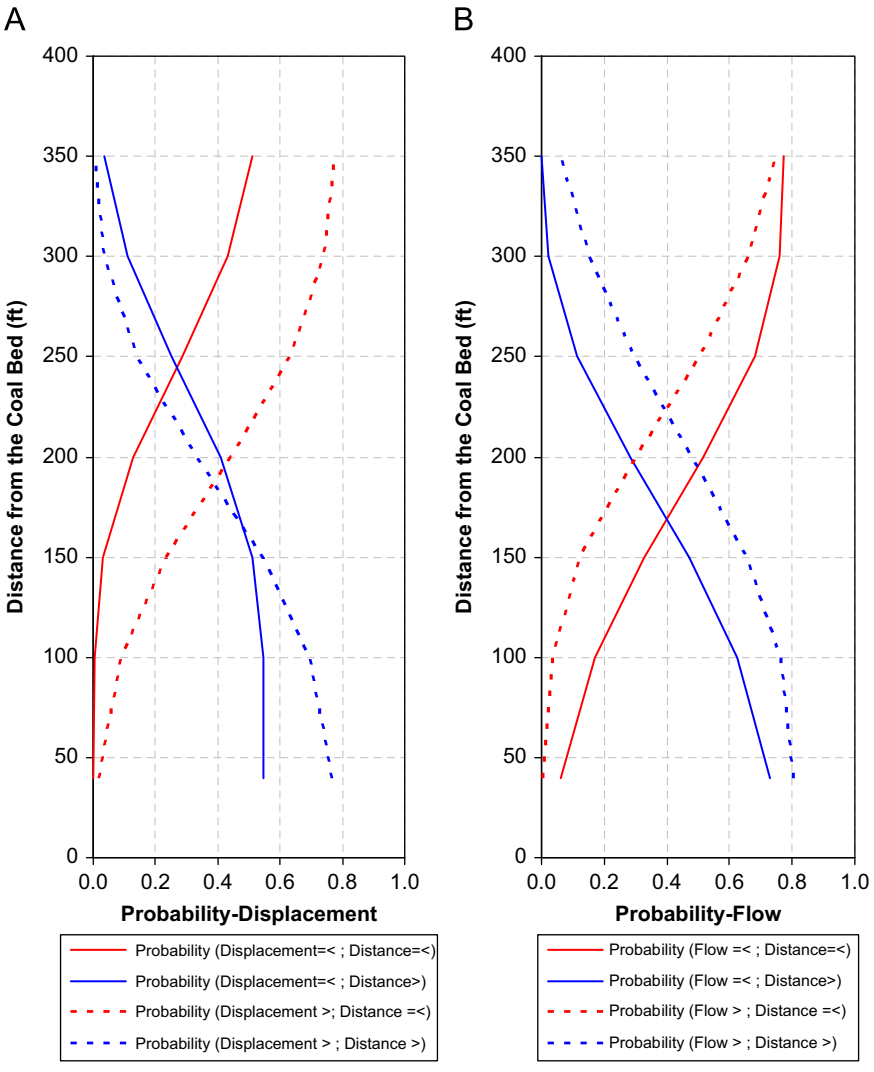

Fig. 11. Graphical representation of conditional probabilities for (a) strata separation and (b) fraction of total flow given in Table 4.

probability of less than 0.8 ft separation occurring. The solid red line in Fig. 11a shows that at most 0.8 ft separation occurs with a probability of 0.8 at a distance of 350 ft from the coal bed and this probability decreases as the distance to the coal bed decreases. The interception of blue and red solid lines gives the probability (~0.25) and the location (~245 ft) of at most a 0.8 ft strata separation.

Fig. 11b shows a similar analysis for the conditional probability of the fraction of total flow entering the borehole at various depths. This figure shows that the probability of at least 0.5 of the total flow entering the borehole below a given height from the coal bed can be traced by the dotted red line. This line shows that this probability is ~0.75 at and below 350 ft, ~0.3 at 200 ft and decreases to almost 0 at and below 50 ft from the coal bed. The intersection of two dotted lines that represent the two sides of this distribution is where at least 0.5 of total flow enters the borehole. This probability is ~0.4 and occurs at 225 ft from the coal bed. On the other hand, the probability of at most 0.9 of total flow entering the borehole is ~0.8 and occurs at and below 350 ft from the coal bed. The probability of at most this much flow entering the borehole at and below 150 ft is about 0.3. The intersection of two solid lines shows that at most 0.9 of total flow enters the borehole at a distance of 175 ft above the coal bed with a probability of 0.4.

A similar example application for evaluating the probabilities can be performed for strata thickness/Young's modulus ratio (T/E) and gas content of the overlying strata (GC). In this analysis 10 and 50 ft/GPa were selected as the lower and upper values for the T/E parameter, and 100 and 250 scf/ton were selected as the lower and upper values for strata gas content. The tabulated values of conditional probabilities as a function of distance to coal bed and overburden depth are given in Table 5 and graphically shown in Fig. 12.

Fig. 12a shows that coal measure strata with a T/E ratio of at least 10 can be located at and below 350 ft above the coal bed with a probability of 0.35. The probability of this type of strata decreases when close to the coal bed. The type of strata that this T/E number can indicate may be thin and have a high Young's modulus. These types of formations are usually rare close to the seam. Thus, the probability of this occurrence is low. On the other hand, the probability of strata with a T/E of at most 50 at and below 350 ft is almost 1.0. This probability is 0.7 less than or equal to 200 ft from the coal bed. Increasing distances from the coal bed increases the possibility of thicker coal-measure formations.

Fig. 12b shows the variation of conditional probabilities as a function of overburden depth for the existence of strata with gas amounts of at least 100 scf/ton and of at most 250 scf/ton. This graph shows that gas contents of at least 100 scf/ton are more probable as the depth increases (red dotted line) to 1300 ft. The probability of finding more than 100 scf/ton gas in the strata at depths 1300 ft and less is ~0.7. On the other hand, the

Table 5
Conditional probabilities for strata thickness/Young's modulus ratio (T/E) of more than 10 ft/GPa and less than 50 ft/GPa and strata gas contents (GC) of more than 100 scf/ton and less than 250 for all regions of the bivariate normal distribution as a function of distance from the coal bed and overburden depth.

T/E (ft/GPa) >	Dist. CB (ft) ≤	Probability	GC (scf/ton) >	Overburden (ft) ≤	Probability
10	40	0.034	100	40	0.002
	100	0.087		100	0.025
	150	0.152		150	0.138
	200	0.222		200	0.378
	250	0.282		250	0.577
	300	0.322		300	0.655
	350	0.342		350	0.669
T/E (ft/GPa) ≤	Distance CB (ft) ≤	Probability	GC (scf/ton) ≤	Overburden (ft) ≤	Probability
50	40	0.127	250	40	0.018
	100	0.302		100	0.108
	150	0.502		150	0.354
	200	0.704		200	0.683
	250	0.867		250	0.899
	300	0.968		300	0.955
	350	0.991		350	0.959
T/E (ft/GPa) >	Distance CB (ft) >	Probability	GC (scf/ton) >	Overburden (ft) >	Probability
10	40	0.319	100	40	0.668
	100	0.267		100	0.645
	150	0.202		150	0.527
	200	0.132		200	0.288
	250	0.071		250	0.089
	300	0.031		300	0.014
	350	0.011		350	0.001
T/E (ft/GPa) ≤	Distance CB (ft) >	Probability	GC (scf/ton) ≤	Overburden (ft) >	Probability
50	40	0.914	250	40	0.950
	100	0.740		100	0.874
	150	0.539		150	0.631
	200	0.338		200	0.302
	250	0.174		250	0.085
	300	0.073		300	0.012
	350	0.014		350	0.001

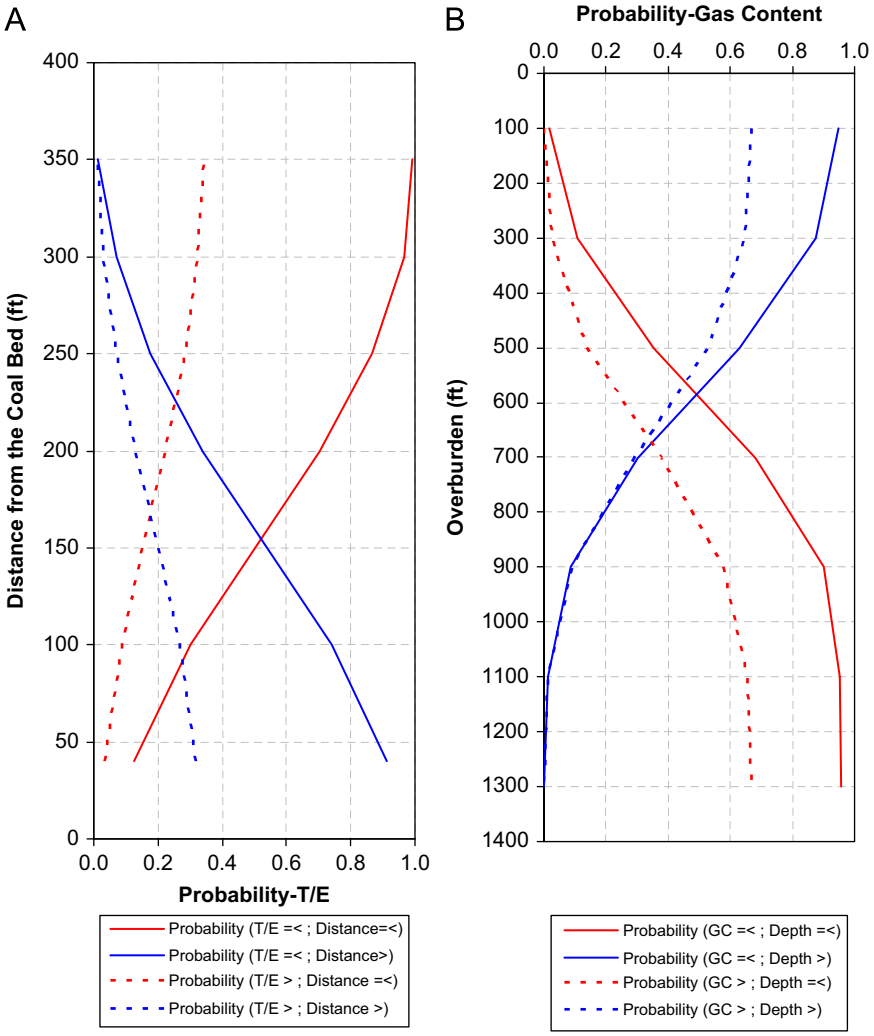

Fig. 12. Graphical representation of conditional probabilities for (a) T/E ratio and (b) strata gas content given in Table 5.

probability of finding gas contents of at most (or less than) 250 scf/ton at the same depth is ~1.0. The intersection of two dotted lines shows that the depth and the probability of encountering a gas content of at least 100 scf/ton are ~650 and ~0.35 ft, respectively.

6. Conclusions

This work presents probabilistic assessments of depth-displacement, depth-flow percentage, depth-formation and depth-gas content relationships using bivariate normal distributions. Using data gleaned from longwall operations in southwestern Pennsylvania and northern West Virginia, joint probabilities were calculated using the bivariate normal distribution. Four-parameter logistic equations were then created to define functional relationships between all data pairs.

Joint and conditional probabilities were developed between strata displacement and distance to coal, inflow and distance to coal, ratio of strata thickness to Young's modulus and distance to coal, and gas content and overburden thickness. Graphical results were presented for displacements of more than 0.3 and less than 0.8 ft, gas inflows of more than 50% and less than 90% of the total flow, ratios of strata thickness to Young's modulus (T/E) of more than 10 ft/GPa and less than 50 ft/GPa, and gas contents of more than 100 scf/ton and less than 250 scf/ton. For instance, the accumulated data suggest that with a probability of approximately 40%, at least 50% of the total methane flow enters a borehole at a location 225 ft above the coalbed. Other data show the probability of occurrence of strata existing with a T/E ratio of at least 10 is 0.35, but decreases with approach to the coalbed. Finally, these results show that the probability of high gas contents of at most 250 scf/ton increases with coalbed depth.

References

[1] Diamond WP. Methane control for underground mines. US Bur Mines Info Circ No 1994;9395:44.
[2] Palchik V. Localization of mining-induced horizontal fractures along rock layer interfaces in overburden: field measurements and prediction. Environ Geol 2005;48:68–80.
[3] Hasenfus GJ, Johnson KL, Su DWH. A hydrogeomechanical study of overburden aquifer response to longwall mining. In: Proceedings of the seventh international conference ground control in mining, Morgantown, WV, 1988.
[4] Cui X, Wang J, Liu Y. Prediction of progressive surface subsidence above longwall coal mining using a time function. Int J Rock Mech Min Sci 2001;38:1057–63.
[5] Karacan CÖ, Goodman GVR. Hydraulic conductivity changes and influencing factors in longwall overburden determined by slug tests in gob gas ventholes. Int J Rock Mech Min Sci 2009;46:1162–74.
[6] Fawcett RJ, Hibberd S, Singh RN. An appraisal of mathematical models to predict water inflows into underground coal workings. Mine Water Environ 1984;3:33–54.

[7] Whittles DN, Lowndes IS, Kingman SW, Yates C, Jobling S. Influence of geotechnical factors on gas flow experienced in a UK longwall coal mine panel. Int J Rock Mech Min Sci 2006;43:369–87.
[8] Whittles DN, Lowndes IS, Kingman SW, Yates C, Jobling S. The stability of methane capture boreholes around a longwall coal panel. Int J Coal Geol 2007;71:313–28.
[9] Ren TX, Edwards JS. Goaf gas modeling techniques to maximize methane capture from surface gob wells. In: De Sauza E, editor. Mine ventilation; 2002. p. 279–86.
[10] Karacan CÖ, Esterhuizen GS, Schatzel SJ, Diamond WP. Reservoir simulation-based modeling for characterizing longwall methane emissions and gob gas venthole production. Int J Coal Geol 2007;71:225–45.
[11] Palchik V. Use of Gaussian distribution for estimation of gob gas drainage well productivity. Math Geol 2002;34:743–65.
[12] Karacan CÖ. Forecasting gob gas venthole production performances using intelligent computing methods for optimum methane control in longwall coal mines. Int J Coal Geol 2009;79:131–44.
[13] Karacan CÖ. Reconciling longwall gob gas reservoirs and venthole production performances using multiple rate drawdown well test analysis. Int J Coal Geol 2009;80:181–95.
[14] Karacan CÖ. Reservoir rock properties of coal measure strata of the Lower Monongahela Group, Greene County (Southwestern Pennsylvania), from methane control and production perspectives. Int J Coal Geol 2009;78:47–64.
[15] Mazza RL, Mlinar MP. Reducing methane in coal mine gob areas with vertical boreholes. US Bur Mines Res Rep 1977. 1607-1-77.
[16] Karacan CÖ. Elastic and shear moduli of coal measure rocks derived from basic well logs using fractal statistics and radial basis functions. Int J Rock Mech Min Sci 2009;48:1281–96.
[17] Diamond WP, La Scola JC, Hyman DM. Results of direct-method determination of the gas content of the US coalbeds. US Bur Mines Info Circ 1986;9067.
[18] Yue S, Ouarda TBMJ, Bobee B. A review of bivariate gamma distributions for hydrological application. J Hydrol 2001;246:1–18.
[19] Krishnamoorty K. Handbook of statistical distributions with applications. Boca Raton: Chapman & Hall/CRC; 2006.
[20] Addinsoft. XL-Stat. version 4.03, 2009. Available from: 〈www.xlstat.com〉.
[21] Gottschalk PG, Dunn JR. The five-parameter logistic: a characterization and comparison with the four-parameter logistic. Anal Biochem 2005;343:54–65.